Journal of Quantitative Spectroscopy & Radiative Transfer ▮ (▮▮▮▮) ▮▮▮–▮▮▮

Contents lists available at ScienceDirect

Journal of Quantitative Spectroscopy & Radiative Transfer

journal homepage: www.elsevier.com/locate/jqsrt

Some improvements of the HNO_3 spectroscopic parameters in the spectral region from 600 to 950 cm^{-1}

L. Gomez [a], H. Tran [a], A. Perrin [a,*], R.R. Gamache [b], A. Laraia [b], J. Orphal [a], P. Chelin [a], C.E. Fellows [c], J.-M. Hartmann [a]

[a] Laboratoire Interuniversitaire des Systèmes Atmosphériques (LISA), UMR 7583, CNRS and Universities Paris Est and Paris 7, 61 Av. Général de Gaulle, 94010 Créteil Cedex, France

[b] Department of Environmental, Earth, and Atmospheric Sciences, University of Massachusetts Lowell and University of Massachusetts, School of Marine Sciences, 265 Riverside Street, University of Massachusetts Lowell, Lowell, MA 01854-5045, USA

[c] Laboratoria de Espectroscopia e Laser, Instituto de Fisica, Universidate Federal Fluminense, Niteroi, Brazil

ARTICLE INFO

Article history:
Received 6 May 2008
Received in revised form
12 July 2008
Accepted 15 July 2008

Keywords:
Nitric acid
Line intensities
Line broadening
Line mixing
Infrared
11.3 μm
nu5+nu6−nu6 band
nu5+nu7−nu7 band
nu5+nu9−nu9 band
nu5 band
2nu9 band
nu8 band
nu6 band
MIPAS
HNO/sub 3/

ABSTRACT

In an earlier study [Flaud JM, Brizzi G, Carlotti M, Perrin A, Ridolfi M. MIPAS database: validation of HNO_3 line parameters using MIPAS satellite measurements. Atmos Chem Phys 2006;6:1–12] the HNO_3 line parameters in the HITRAN spectroscopic database have recently been revisited in the spectral range corresponding to the MIPAS spectral range. For the 11.3 μm, these updates involve the line positions for the $\{\nu_5, 2\nu_9\}$ bands, and the intensities. However, comparisons between observed spectra recorded by MIPAS and the calculated ones in the 600–950 cm^{-1} region still show significant disagreements. The goal of the present paper is to solve some of these problems. Based on the analysis of N_2-broadened HNO_3 laboratory spectra recorded with a Fourier transform instrument, a new HNO_3 database was generated, including the following improvements: (i) approximate parameters for the $\nu_5+\nu_7-\nu_7$ and $\nu_5+\nu_6-\nu_6$ hot bands have been added, and (ii) the intensities for the ν_6 and ν_8 bands have been updated. (iii) The air broadening and its temperature dependence, calculated using a semi-classical approach, have been added for each HNO_3 transition. (iv) Finally, line-mixing effects have been pointed out, particularly in the $\nu_5+\nu_9-\nu_9$ Q branch, and an approach correctly modeling the resulting spectral shape is proposed.

1. Introduction

Nitric acid plays an important role in atmospheric chemistry since it acts as a reservoir of NO_x, which are directly involved in ozone destruction [1]. HNO_3 is observed in operational mode by the "Michelson Interferometer for Passive Atmospheric Sounding" (MIPAS) on board the EnviSat satellite [2], for instance. The 11.3 μm region is widely used for the remote sensing of vertical distribution of HNO_3 [3–5] since it is located in an atmospheric window and contains strong absorption bands, namely the ν_5 and $2\nu_9$ cold bands located at 879 and 896 cm^{-1} together with the associated $\nu_5+\nu_9-\nu_9$ and $3\nu_9-\nu_9$ first hot bands at 885 and 830 cm^{-1} [6].

* Corresponding author. Tel.: +33 145176557; fax: +33 145171564.
E-mail address: perrin@lisa.univ-paris12.fr (A. Perrin).

0022-4073/$ - see front matter © 2008 Published by Elsevier Ltd.
doi:10.1016/j.jqsrt.2008.07.004

In an earlier study [7] the HNO_3 spectroscopic parameters available in the HITRAN [8] and GEISA [9] databases have been revisited in the spectral region covered by MIPAS spectra. The line positions were improved in the 11.3 and 8.3 μm regions using new parameters determined in Refs. [10,11]. The line intensities were also updated, mainly based on the integrated absorption cross-section measurements performed in the 820–5300 cm^{-1} region by Chackerian et al. [12]. Finally, the line-broadening coefficients were also changed from the line-independent values provided in the former versions of the data bases. The most accurate HNO_3 line-broadening measurements were performed in the microwave or submillimeter spectral regions [13–18], where, contrary to the infrared, isolated lines can be observed. These measurements clearly evidence a rotational dependence of the air-broadening coefficients. In the absence of accurate theoretical calculation at that time, it was decided to rely on a simple empirical model (see Ref. [19] for details) that reproduces as well as possible the measured values of the line-broadening parameters.

For the 11.3 μm region (840–930 cm^{-1}), the residuals between atmospheric spectra recorded by MIPAS and those calculated using these new parameters [7] are considerably reduced when compared with results obtained using the previous line parameters available in HITRAN [8]. For this reason, these new parameters are now implemented in the updated version of the databases. However, when examining in details the results of these comparisons (see, for example, Figs. 1 and 2 of Ref. [7]) some significant features can be still observed in the residuals. The goal of the present paper is to further investigate nitric acid absorption in order to improve spectra calculations and correct for some of the observed discrepancies. For this purpose, several laboratory spectra of nitric acid broadened by N_2 (total pressures from 88 to 1019 hPa; see Section 3.2) have been recorded at room temperature using the Bruker IFS 125HR Fourier transform spectrometer (FTS) of the LISA laboratory. These are used to test the quality of the current spectroscopic list, first using Voigt line shapes. These comparisons evidence various discrepancies so that four modifications have been made in order to improve the [7] line list: (1) we have added line parameters for the $\nu_5+\nu_7-\nu_7$ and $\nu_5+\nu_6-\nu_6$ hot bands, which were not included in the previous line list. (2) The spectral range covered by the present study (600–950 cm^{-1}) includes the weak ν_6 and ν_8 bands. These bands, which were not considered in the line intensity study performed in Ref. [12], were not updated in the new HITRAN line list. From the present study we have observed that the intensities in HITRAN for the ν_6 and ν_8 bands are not consistent with those of ν_5 and $2\nu_9$. More explicitly their intensities are overestimated by about 20–30%, and we thus propose values for these intensities. (3) Following recent line-broadening calculations [20] the air-broadening parameters were updated. (4) Finally, we propose a model for line-mixing effects in HNO_3 spectra. Its validity is demonstrated, particularly in the narrow Q branches of the $\nu_5+\nu_9-\nu_9$ and ν_8 bands, which cannot be modeled at all pressures using Voigt isolated line shapes.

2. Experimental measurements

High-resolution infrared absorption spectra of HNO_3/N_2 mixtures were recorded using the Bruker IFS 125HR (an upgraded version of the IFS 120HR) FTS of LISA in Créteil. A glowbar source was used, together with a KBr beamsplitter with a dichroic coating and a MCT detector, in order to cover the 500–5200 cm^{-1} spectral range. The FTS was evacuated to about 0.05 hPa in order to reduce the absorption by laboratory air. Pressures were measured using calibrated MKS Baratron pressure transducers. The optical path difference used was 38 cm, leading to a spectral resolution of 0.013 cm^{-1} (boxcar apodization), and, for each HNO_3/N_2 mixture, 50 individual scans were recorded. This leads to a measurement time of about 20 min, short enough to make sure that the HNO_3 concentration in the absorption does not vary significantly between the first and last scans.

The White-type multipass absorption cell, made of pyrex glass and equipped with wedged CsI windows, was connected to the FTS with a dedicated optical interface (six mirrors) inside the sample chamber of the FTS. Its base length is 0.80 m, and, for the experiments described here, an optical path of 9.60 m was used, in order to work with low HNO_3 partial pressures (even if they are not exactly experimentally determined) and to eliminate any self-broadening effects.

In order to obtain a stable HNO_3 sample entirely free of NO_2, the reaction of N_2O_5 with H_2O in the presence of O_3 was used. In addition, to avoid other impurities, the White cell was first chemically cleaned using about 10 hPa of a mixture of 1% O_3 in O_2 (produced with a commercial discharge-based ozonizer, Sander Germany) that was filled into the absorption cell during one night. Second, we evacuated the absorption cell and filled it with about 0.2 hPa of pure NO_2 (Sigma Aldrich).

Third, we added about 100 hPa of a mixture of O_3/O_2, which leads to the immediate production of N_2O_5 (through the reaction of NO_2 with O_3 producing NO_3 [21]), followed by the slow production of HNO_3 (by the heterogeneous reaction of N_2O_5 with residual H_2O on the walls of the absorption cell). All these reactions were monitored by recording low-resolution infrared absorption spectra. In order to complete the last reaction, the mixture was left in the absorption cell for another night. Finally, the total pressure in the absorption cell was reduced to about 5 hPa in order to achieve the desired HNO_3 absorption, and dry nitrogen (Air Liquide France) was added up to a total pressure of about 1 atm. The presence of some O_3 in the mixture guaranteed that any NO_2 produced from HNO_3 photolysis or decomposition would react back to NO_3 and then to HNO_3. Indeed, no residual NO_2 absorption is observed in the spectra.

Starting from the HNO_3/N_2 mixture, eight spectra were recorded at total pressures of 1019, 885, 754, 624, 489, 356, 223, and 88 hPa by progressively evacuating the cell. Before and after this procedure, spectra of the empty cell were recorded. Also note that the spectrum recorded with a high concentration of HNO_3 (after the filling of the cell with NO_2 and an O_3/O_2

Please cite this article as: Gomez L, et al. Some improvements of the HNO_3 spectroscopic parameters in the spectral region from 600 to 950 cm^{-1}. JQSRT (2008), doi:10.1016/j.jqsrt.2008.07.004

mixture in the second step) allows for determination of the zero-transmittance baseline that can be slightly different from zero due to detector non-linearity.

3. Extended database and line-mixing model

3.1. Hot bands addition

Two (unidentified) Q-type structures located at 869.1 and 875.7 cm^{-1}, respectively, are observed in our measured spectra. These wavenumbers correspond very closely to the differences between the measured positions of the $\nu_5+\nu_6$

Table 1
Summary of the HNO_3 bands on this new database

Band	Band center (cm^{-1})	S_{TOT} (cm^{-1}/molc cm^{-2})	S_{min} (cm^{-1}/molc cm^{-2})	S_{max} (cm^{-1}/molc cm^{-2})	Number of lines	σ_{min} (cm^{-1})	σ_{max} (cm^{-1})
ν_5	879.108	1.027 E−17	9.83 E−25	6.60 E−21	57,108	806.207	963.995
ν_6	646.826	1.263 E−18	2.83 E−23	8.54 E−22	8379	615.026	677.981
ν_6 (updated)	646.826	9.342 E−19	2.09 E−23	6.32 E−22	8379	615.026	677.981
ν_8	763.154	1.242 E−18	1.21 E−23	1.09 E−21	7101	722.533	809.965
ν_8 (updated)	763.154	9.689 E−19	9.45 E−24	8.50 E−22	7101	722.533	809.965
$2\nu_9$	896.447	7.503 E−18	9.83 E−25	3.88 E−21	55,310	806.709	963.435
$\nu_5+\nu_6-\nu_6$ (new)	869.1	6.179 E−19	5.92 E−26	3.97 E−22	57,108	796.207	953.995
$\nu_5+\nu_7-\nu_7$ (new)	875.7	9.760 E−19	9.35 E−26	6.27 E−22	57,108	802.807	960.595
$!\nu_9-\nu_9$	830.675	5.291 E−19	3.84 E−25	6.72 E−22	17,720	769.687	884.438
$\nu_3+\nu_9-\nu_9$	885.425	1.067 E−18	9.87 E−25	7.00 E−22	14,521	832.117	942.901

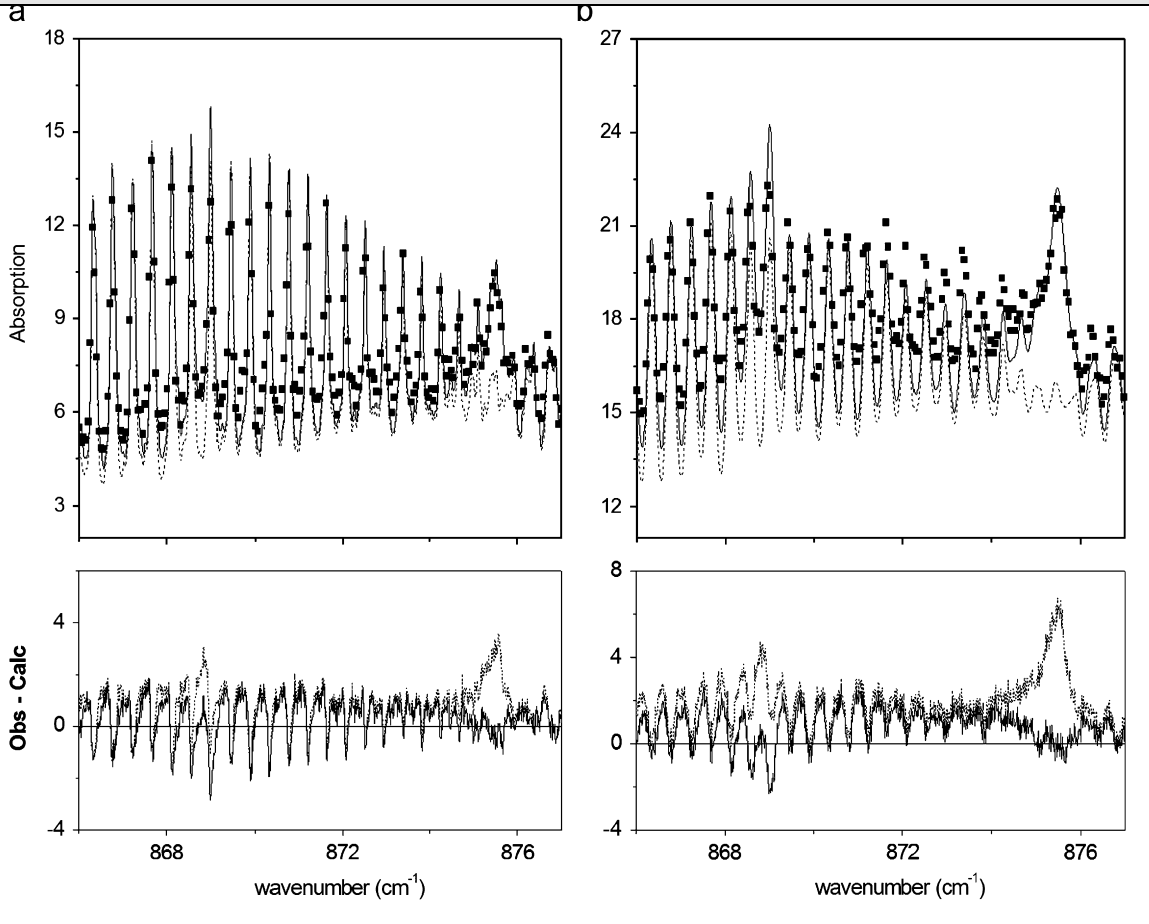

Fig. 1. Absorption coefficients measured (■) and calculated with (—) and without (- - -) the addition of the $\nu_5+\nu_6-\nu_6$ and $\nu_5+\nu_7-\nu_7$ hot bands for a temperature of 296 K and a total pressure of (a) 356 hPa and (b) 1019 hPa. The curves in the lower layers are corresponding deviations (obs–calc).

Please cite this article as: Gomez L, et al. Some improvements of the HNO_3 spectroscopic parameters in the spectral region from 600 to 950 cm^{-1}. JQSRT (2008), doi:10.1016/j.jqsrt.2008.07.004

(1521 cm^{-1}) and $\nu_5+\nu_7$ (1455 cm^{-1}) bands [22] and the energies of the ν_6 (646.826 cm^{-1}) and ν_7 (580.304 cm^{-1}) levels [23]. We thus propose $\nu_5+\nu_6-\nu_6$ and $\nu_5+\nu_7-\nu_7$ for the assignments of the 869.1 and 875.7 cm^{-1} structures, respectively, since other possibilities can be eliminated. If we consider the case for the ν_5 and $2\nu_9$ bands of one of the minor isotopic variants of nitric acid, for example, we must take into account that the most abundant isotope variant $H^{15}NO_3$, (with a relative abundance of 0.00364) ν_5 and $2\nu_9$ were already identified at 871.0955 and 893.4518 cm^{-1}, respectively [24], where we cannot distinguish any structure in our spectra, and the other isotopic variants are not abundant enough (0.0019 and 0.0003 for the isotopic variants in ^{18}O and D, respectively [25]) to be considered here. Other possible candidates for such assignments are hot bands of the main isotopic species. The rather strong $\nu_5+\nu_9-\nu_9$ and the significantly weaker $3\nu_9-\nu_9$, first hot bands at 885 and 830 cm^{-1}, can be disregarded since they are already present in line lists (see Table 1). Finally, the $2\nu_9+\nu_x-\nu_x$ series of hot bands are expected to be considerably weaker than the $\nu_5+\nu_x-\nu_x$ first series. Indeed, as for $2\nu_9$, the $2\nu_9+\nu_x-\nu_x$ bands correspond to a difference of $\Delta\nu_9=\pm2$ in the ν_9 vibrational quantum number, and these overtones transitions are expected to be very weak. However, one should mention that, in the particular case of $H^{14}NO_3$, the $2\nu_9$ band is intense since it borrows most of its intensity from the strong ν_5 band. This is due to a Fermi-type resonance between the 5^1 and 9^2 vibrational levels, which is strong since the unperturbed vibrational states are very close in energy (only 7 cm^{-1} of separation) [11]. In principle, a similar Fermi resonance may also affect the $\nu_5+\nu_x$ and $2\nu_9+\nu_x$ states but it is expected to be weak due to the likely much larger energy separation between these levels. Finally, note that, as can be seen in Table 1, the $\nu_5+\nu_6-\nu_6$ and $\nu_5+\nu_7-\nu_7$ assignments are also consistent with intensity considerations. Indeed, since $E_7<E_6$ the $\nu_5+\nu_7-\nu_7$ band, having a more populated lower level, is stronger than the $\nu_5+\nu_6-\nu_6$ one.

In the absence of high-resolution data for the $\nu_5+\nu_6$ and $\nu_5+\nu_7$ bands, approximate line parameters for the two hot bands have been deduced from those of the ν_5 band. The position $\sigma_{\nu_5+\nu_x-\nu_x}(J,K_a,K_c\leftarrow J'',K_a'',K_c'')$ of a given transition of the $\nu_5+\nu_x-\nu_x$ ($x=6$ or 7) is deduced by applying a shift $-\delta_x$ to the position $\sigma_{\nu_5}(J,K_a,K_c\leftarrow J'',K_a'',K_c'')$ of the corresponding transition in ν_5 band, i.e.:

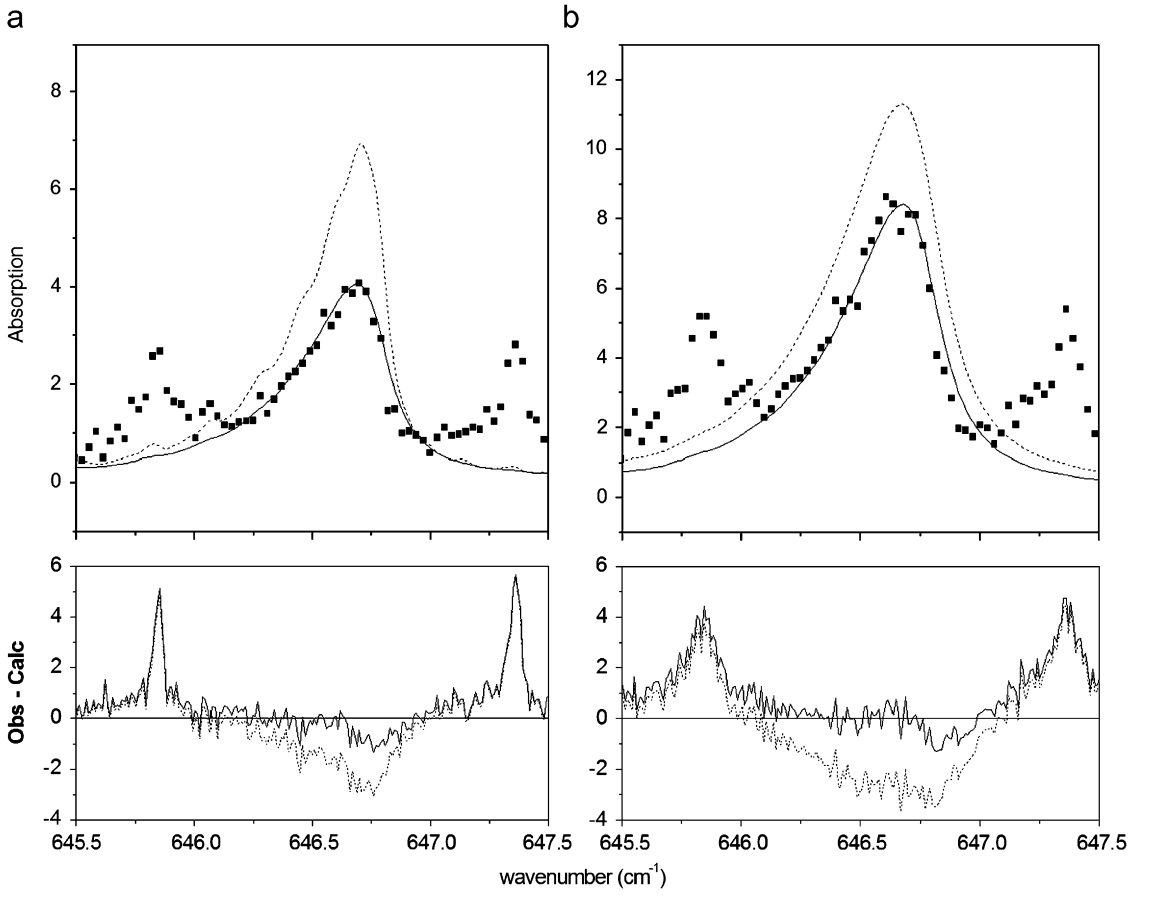

Fig. 2. Absorption coefficients measured (■) and calculated multiplying (—) and not multiplying (- - -) the intensities of ν_6 band in HITRAN database by a factor of 0.74, for a temperature of 296 K and a total pressure of (a) 356 hPa and (b) 1019 hPa. The curves in the lower layers are corresponding deviations (obs–calc).

Please cite this article as: Gomez L, et al. Some improvements of the HNO_3 spectroscopic parameters in the spectral region from 600 to 950 cm^{-1}. JQSRT (2008), doi:10.1016/j.jqsrt.2008.07.004

$$\sigma_{v_5+v_x-v_x}(J,K_a,K_c \leftarrow J'',K_a'',K_c'') = \sigma_{v_5}(J,K_a,K_c \leftarrow J'',K_a'',K_c'') - \delta_x, \quad (1)$$

with the values $\delta_6 = 10.0(\pm 0.5)\ \mathrm{cm}^{-1}$ and $\delta_7 = 3.4(\pm 0.2)\ \mathrm{cm}^{-1}$ determined from the measured spectra.

For an *isolated* band, the intensity $S(v_n+v_x-v_x)$ of an individual rotational transition $v_n+v_x,J,K_a,K_c \leftarrow v_x,J'',K_a'',K_c''$ of the $v_n+v_x-v_x$ hot band can be approximated from the corresponding intensity $S(v_n)$ of the similar rotational transition $v_n,J,K_a,K_c \leftarrow \text{ground},J'',K_a'',K_c''$ of the cold v_n band by simply applying a Boltzmann population factor, i.e.:

$$S(v_n+v_x-v_x) = S(v_n)\exp\left(\frac{-hcE_x}{k_B T}\right), \quad (2)$$

where h is the Planck constant, c is the light speed, E_x is the vibrational band center for the v_x band, k_B is the Boltzmann constant, and T the temperature. In the case of the $v_5+v_6-v_6$ and $v_5+v_7-v_7$ hot bands of $H^{14}NO_3$, this expression must be modified. Indeed, through the $5^1 \Leftrightarrow 9^2$ Fermi resonance, there is a partial transfer of intensity from the v_5 to the $2v_9$ band. In order to take this effect into account, the individual line intensities of the $v_5+v_6-v_6$ and $v_5+v_7-v_7$ transitions are written as

$$S(v_5+v_x-v_x) = S(v_5)\exp\left(\frac{-hcE_x}{k_B T}\right) f_x \quad (3)$$

with $x = 6,7$. The f_6 and f_7 factors were adjusted on the observed spectra, leading to $f_6 = 1.4(\pm 0.2)$ and $f_7 = 1.6(\pm 0.2)$. These values are greater than unity since the 5^1+x^1 and 9^2+x^1 (unknown) vibrational states are (likely) further apart that 5^1 and 9^2 so that the transfer of intensities is weaker than for the cold bands.

Table 1 summarizes the characteristics of the line lists which were generated for the $v_5+v_6-v_6$ and $v_5+v_7-v_7$ hot bands. Fig. 1 displays two observed spectra and corresponding simulations performed with the original HITRAN line parameters available and with those of our new database including the $v_5+v_6-v_6$ and $v_5+v_7-v_7$ hot bands. It is clear that the quality of the simulation in the 869–876 cm^{-1} region is significantly improved.

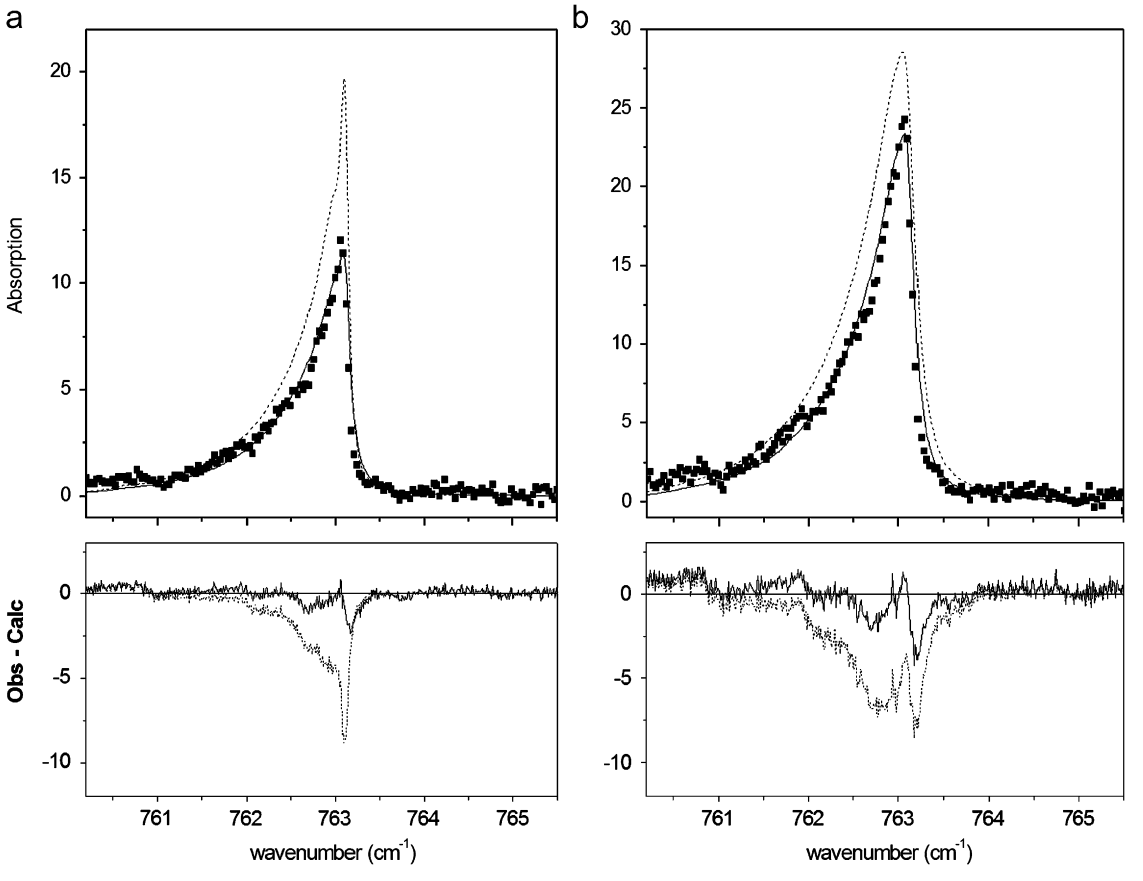

Fig. 3. Absorption coefficients measured (■) and calculated multiplying (—) and not multiplying (- - -) the intensities of v_8 band in HITRAN database by a factor of 0.78, for a temperature of 296 K and a total pressure of (a) 356 hPa and (b) 1019 hPa. The curves in the lower layers are corresponding deviations (obs–calc).

Please cite this article as: Gomez L, et al. Some improvements of the HNO_3 spectroscopic parameters in the spectral region from 600 to 950 cm^{-1}. JQSRT (2008), doi:10.1016/j.jqsrt.2008.07.004

3.2. Calibration of the ν_6 and ν_8 bands' intensities

Our measured spectra enable a test of the relative consistency of the HNO_3 line intensities in the whole 600–950 cm^{-1} spectral region. In order to do this, the unknown HNO_3 amount in our experiments is determined from the absorption in the 11.3 μm region (i.e., ν_5, $2\nu_9$, and associated hot bands). This is valid, since the associated line intensity parameters were recently accurately updated [7] by using the results of the exhaustive measurements of nitric acid integrated absorption cross sections performed in Ref. [12]. However, the low frequency range 600–820 cm^{-1}, which is not covered by the measurements of Ref. [12], was not updated. For the ν_6 and ν_8 bands at 646.826 and 763.154 cm^{-1}, respectively, the line intensities presently available in HITRAN [26] have been scaled to the band intensity measurements of Ref. [27]. The question of the consistency of the line intensities is of relevance. It is further justified by the fact that, from Ref. [28], it was concluded that the ν_6 and ν_8 intensities in HITRAN database [26] are overestimated by a factor of about two. Finally, note that the line positions were slightly improved in Refs. [29,30] for the P and R branches of the ν_6 and ν_8 bands, respectively, but not for the Q branches.

The inadequacy of the ν_6 and ν_8 intensities in HITRAN is confirmed by the present study where scaling factors (with respect to the HITRAN values) of 0.74 and 0.78 have been deduced for the ν_6 and ν_8 bands, respectively. This leads to significantly improved agreement with measured spectra, as shown in Figs. 2 and 3. Note that the two strong peaks in the residuals of Fig. 2 are due to CO_2 lines of the ν_2 band (from small CO_2 impurities in the N_2 used for the experiments).

3.3. New line-broadening parameters

New accurate γ_{air} air-broadening parameters for HNO_3 were introduced in our spectroscopic line list. They result from semi-classical calculations for HNO_3–N_2 performed by Gamache and co-workers following a method based on the complex Robert–Bonamy formalism. Details of these calculations can be found in Ref. [20]. The $\gamma_{air}/\gamma_{N_2} = 0.935$ ratio was estimated using the experimental values of γ_{N_2} and γ_{O_2} (O_2-broadening parameters) of Refs. [13–17].

3.4. Line-mixing effects

At this step, we have built an improved (approximate) database for HNO_3 line parameters in the region from 600 to 950 cm^{-1}, which is more complete and precise than that of [7]. The remaining point studied here is line mixing [31], which is restricted to the Q branches of strong bands since, in the pressure range considered, this process negligibly affects P and R branches. The approach used here is similar to that of Refs. [32,33]. We assume the impact approximation and binary collisions and neglect Doppler effects which are much smaller than the collisional broadening in the studied pressure range. The absorption coefficient, α, in cm^{-1}, for HNO_3 perturbed by N_2 accounting for line-mixing effects at wavenumber σ and temperature T is then given by

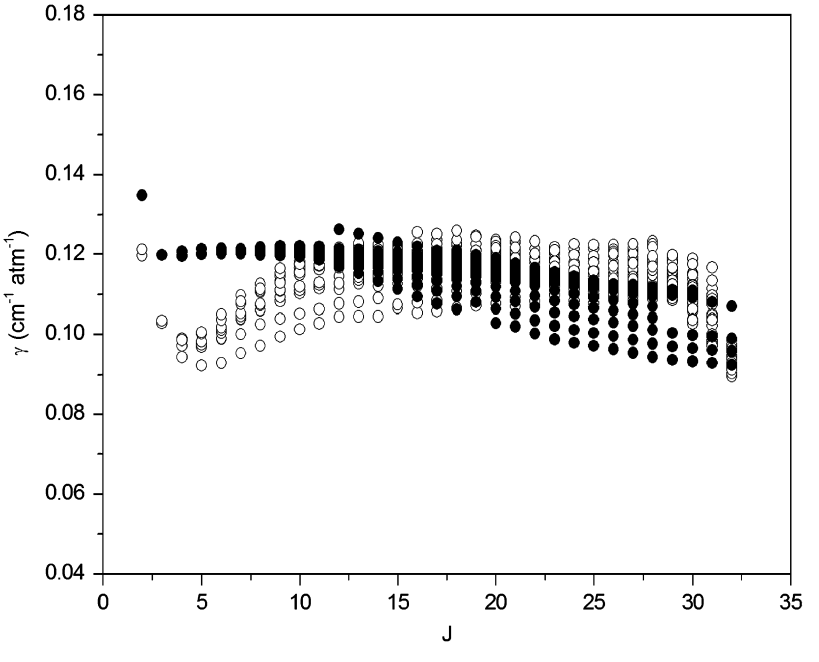

Fig. 4. Q branch line broadening coefficients of HNO_3 perturbed by N_2 in function of J. The open symbols correspond to calculated values (see text) and the full symbols to PEGL fit (Eqs. (8)–(11)).

Please cite this article as: Gomez L, et al. Some improvements of the HNO_3 spectroscopic parameters in the spectral region from 600 to 950 cm^{-1}. JQSRT (2008), doi:10.1016/j.jqsrt.2008.07.004

$$\alpha^{\mathrm{LM}}(\sigma, P_{\mathrm{HNO_3}}, P, T) = \frac{8\pi^3\sigma}{3hc}[1-\exp(-hc\sigma/k_{\mathrm{B}}T)] \times \frac{P_{\mathrm{HNO_3}}}{k_{\mathrm{B}}T} \times \frac{1}{\pi}\mathrm{Im} \times \left\{ \sum_{\ell}\sum_{\ell'} \rho_{\ell}(T) d_{\ell} d_{\ell'} \langle\langle \ell' \| [\mathbf{\Sigma} - \mathbf{L_0} - \mathrm{i}\, P\, \mathbf{W}(T)]^{-1} \| \ell \rangle\rangle \right\}, \quad (4)$$

where the summation is over all ℓ and ℓ' absorption lines. $P_{\mathrm{HNO_3}}$ and P are, respectively, the HNO_3 partial pressure and the total pressures, P thus being the N_2 pressure since HNO_3 is highly diluted. $\mathbf{\Sigma}$, $\mathbf{L_0}$ and $\mathbf{W}$ are operators in the Liouville line space, ρ_{ℓ} is the relative population of the initial level of the line ℓ, d_{ℓ} is the matrix element of the electric dipole moment operator for line ℓ. The latter is related to the integrated intensity S_{ℓ} by the expression:

$$S_{\ell}(T) = \frac{8\pi^3}{3hc}\rho_{\ell}(T) \times \sigma_{\ell} \times \left[1-\exp(hc\sigma_{\ell}/k_{\mathrm{B}}T)\right] \times d_{\ell}^2 \quad (5)$$

$\mathbf{\Sigma}$ and $\mathbf{L_0}$ are diagonal with elements related to the current wavenumber σ and the line positions σ_{ℓ} by

$$\langle\langle \ell | \mathbf{\Sigma} | \ell' \rangle\rangle = \sigma \times \delta_{\ell,\ell'}, \quad \langle\langle \ell | \mathbf{L_0} | \ell' \rangle\rangle = \sigma_{\ell} \times \delta_{\ell,\ell'}. \quad (6)$$

$\mathbf{W}$ is the relaxation operator which off-diagonal elements account for the interferences between absorption lines (line mixing), whereas the real and imaginary parts of the diagonal ones are the collisional-broadening and shifting coefficients, γ_{ℓ} and δ_{ℓ}, respectively, i.e.:

$$\langle\langle \ell | \mathbf{W}(T) | \ell \rangle\rangle = \gamma_{\ell}(T) - \mathrm{i}\delta_{\ell}(T). \quad (7)$$

The pressure shifting coefficients, expected to be very small [18], are considered as negligible in the pressure range considered in this work and the entire imaginary part of $\mathbf{W}$ is therefore neglected. The real-valued off-diagonal elements are modeled using the state-to-state inelastic collisional rates of the lower states as

$$\langle\langle \ell' | \mathbf{W}(T) | \ell \rangle\rangle = -A_{\ell',\ell} \times K(i_{\ell'} \leftarrow i_{\ell}, T), \quad \text{with } (\ell' \neq \ell), \quad (8)$$

where $K(i_{\ell'} \leftarrow i_{\ell}, T)$ is the collisional transfer rate from the initial level i_{ℓ} of line ℓ to the initial level $i_{\ell'}$ of the line ℓ'. The empirical $A_{\ell',\ell}$ parameters which relate state-space to line-space quantities are empirical and depend, strictly speaking, on the lines considered. In order to simplify the problem, we assume that $A_{\ell',\ell}$ depends only on the type of the considered

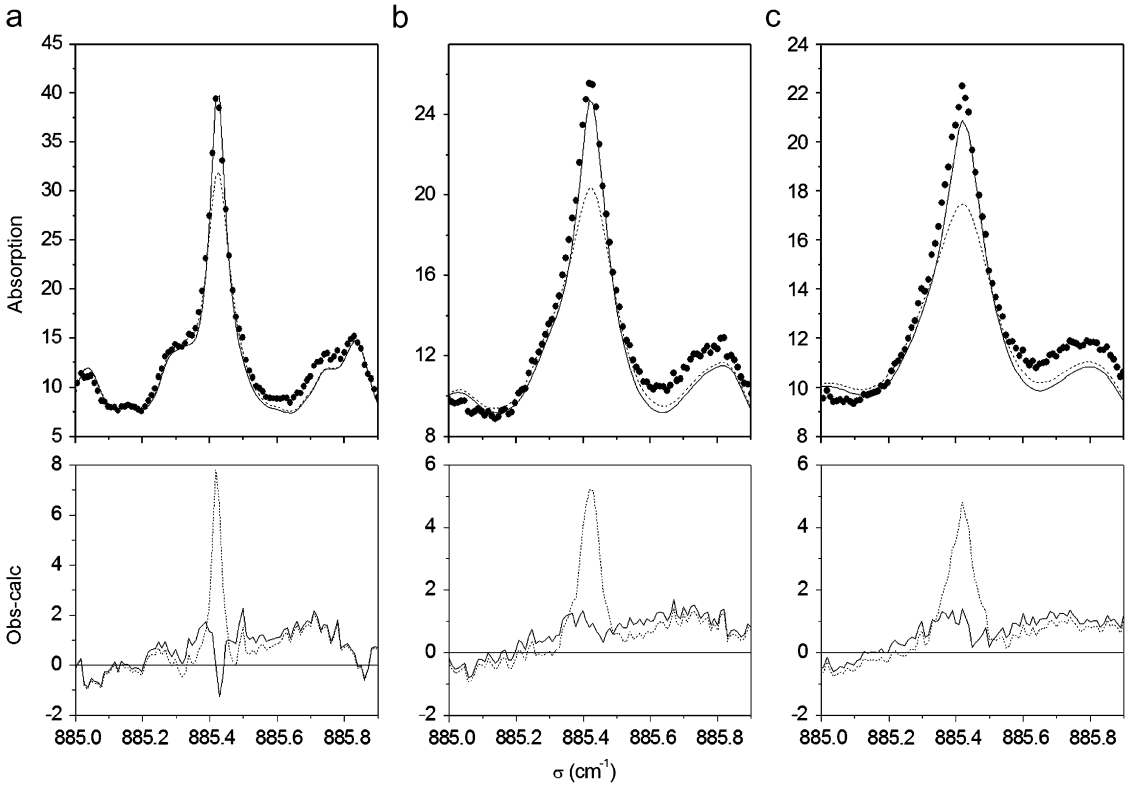

Fig. 5. Absorption coefficients measured (●) and calculated with (—) and without (- - -) line-mixing effects in the region of the $\nu_5+\nu_9-\nu_9$ hot band for a temperature of 296 K and a total pressure of (a) 356 hPa, (b) 754 hPa, and (c) 1019 hPa. The curves in the lower layers are corresponding deviations (obs–calc).

Please cite this article as: Gomez L, et al. Some improvements of the HNO_3 spectroscopic parameters in the spectral region from 600 to 950 cm^{-1}. JQSRT (2008), doi:10.1016/j.jqsrt.2008.07.004

band. The downward rates $K(i_{\ell'} \leftarrow i_\ell, T)$, with $E_{\ell'} < E_\ell$, are modeled by an Exponential Power Gap fitting Law (EPGL) [33]:

$$K(i_{\ell'} \leftarrow i_\ell, T) = a_1 \left(\frac{hc|E_\ell - E_{\ell'}|}{k_B T} \right)^{-a_2} \exp\left(-\frac{a_3 hc|E_\ell - E_{\ell'}|}{k_B T} \right). \quad (9)$$

The upward ones have been deduced from the following detailed balance relation:

$$K(i_\ell \leftarrow i_{\ell'}, T) = \frac{\rho_\ell(T)}{\rho_{\ell'}(T)} K(i_{\ell'} \leftarrow i_\ell, T). \quad (10)$$

The a_1, a_2, and a_3 coefficients are obtained from least-squares fits of the collisional-broadening coefficients γ_k using the following sum rule applied for a Q branch:

$$\gamma_\ell = \sum_{\ell' \neq \ell} K(i_{\ell'} \leftarrow i_\ell). \quad (11)$$

For the Q branches considered in this work (ν_5, $2\nu_9$, $\nu_5+\nu_9-\nu_9$, ν_8), due to symmetry considerations, only rates connecting rotational levels with the selection rule ΔK_c odd, are non zero. Imposing this and using Eqs. (9)–(11) for a fit of line-broadening values leads to the following parameters for the EPGL fitting law: $a_1 = 0.00117$, $a_2 = 0.015$, $a_3 = 13.95$ and to the results of Fig. 4. The agreement is not perfect but still reasonable. The final parameters A of Eq. (8) have then been determined from fits of the experimental spectrum for $P = 1019$ hPa. They are $A = 0.5$ and $A = 0.3$ for type A (ν_5, $2\nu_9$, $\nu_5+\nu_9-\nu_9$) and type C (ν_8) bands, respectively.

As a first example, comparisons between measurements and calculations for the Q branch of the hot band $\nu_5+\nu_9-\nu_9$ at different pressures are shown in Fig. 5. As can be expected [31], Lorentzian line shapes strongly underestimate peak absorption, whereas overestimates the Q branch width. On the opposite, our model leads to significant improvement and satisfactory agreement, demonstrating that line mixing must be accounted for in the $\nu_5+\nu_9-\nu_9$ Q branch. On the contrary, no appreciable line-mixing effects are detected for the ν_5 and $2\nu_9$ Q branches since their lines are more widely spread

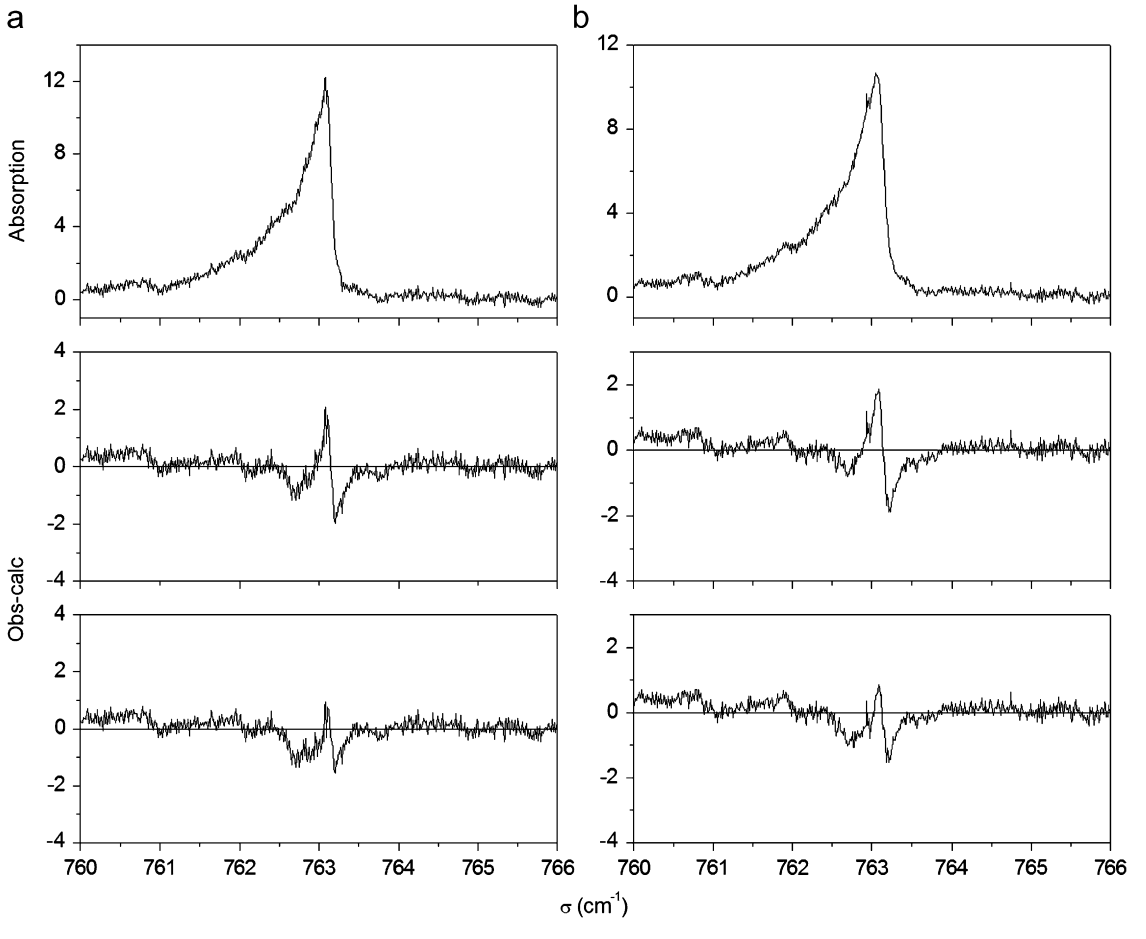

Fig. 6. In the top: absorption measured in the region of the ν_8 band for a temperature of 296 K and a total pressure of (a) 754 hPa and (b) 1019 hPa. The curves in the medium and the lower layers are, respectively, the differences between measured spectra and calculations without and with line-mixing effects.

Please cite this article as: Gomez L, et al. Some improvements of the HNO_3 spectroscopic parameters in the spectral region from 600 to 950 cm^{-1}. JQSRT (2008), doi:10.1016/j.jqsrt.2008.07.004

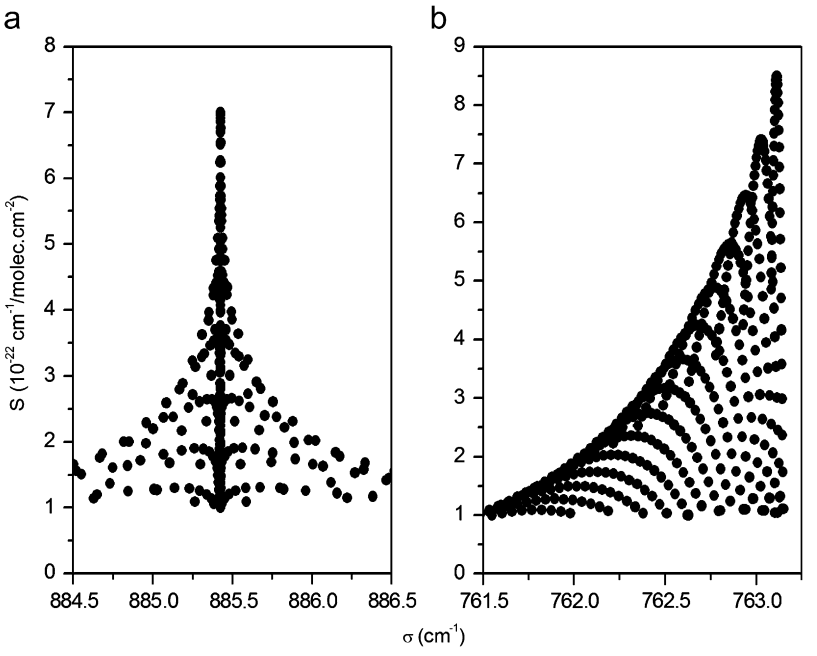

Fig. 7. Intensities of the (a) $\nu_5+\nu_9-\nu_9$ and (b) ν_8 Q branches lines deducted from our new database.

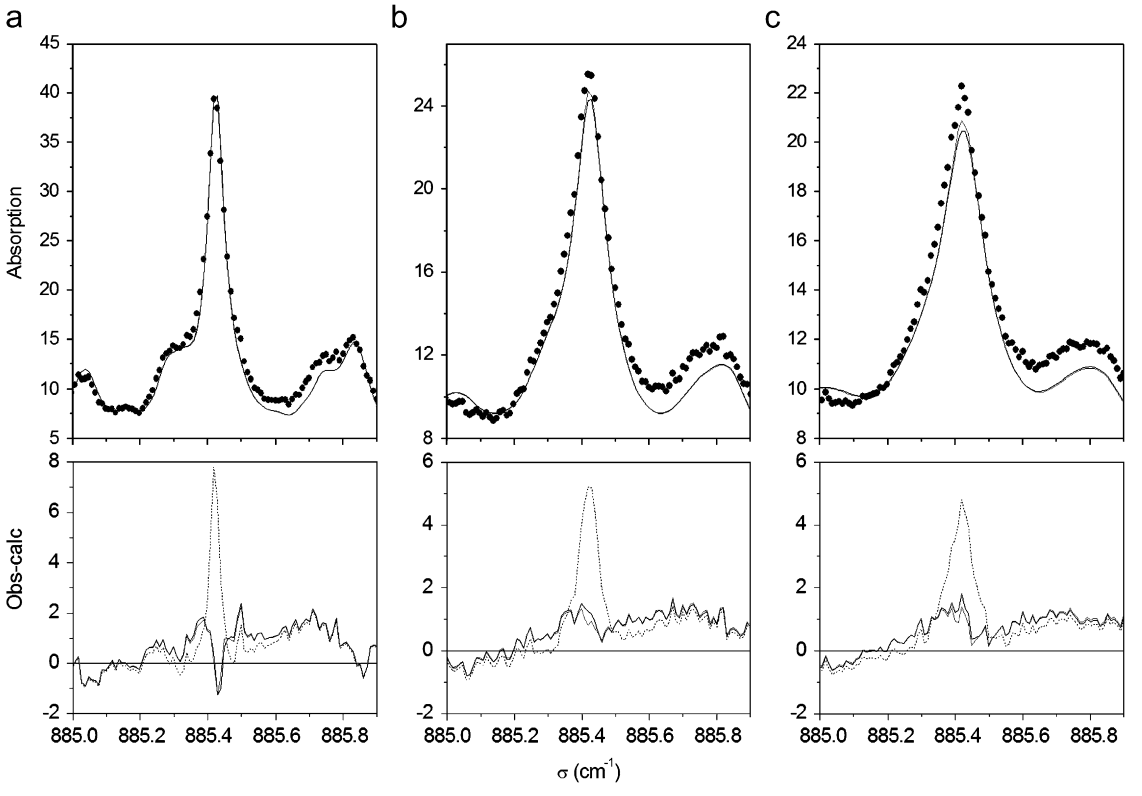

Fig. 8. Same experimental conditions as in Fig. 3 but the comparisons are between measurements (black points) and calculation accounting for line-mixing effects using our model (grey line) and using equivalent Lorentzian line shapes (black line). The (obs–calc) corresponding values are plotted in the lower layers. Differences between measurements and calculation without line-mixing effects (dash) are also reported for comparison.

Please cite this article as: Gomez L, et al. Some improvements of the HNO_3 spectroscopic parameters in the spectral region from 600 to 950 cm^{-1}. JQSRT (2008), doi:10.1016/j.jqsrt.2008.07.004

[11,34]. Finally, results obtained for the ν_8 Q branch are shown in Fig. 6 where line-mixing effects are detected but are significantly weaker than that of the $\nu_5+\nu_9-\nu_9$ Q branch.

In order to simplify the practical inclusion of line-mixing effects in atmospheric computation codes, a simple approach is proposed. It consists of calculating the profiles of the $\nu_5+\nu_9-\nu_9$ and ν_8 Q branches using Lorentzian line shapes with ad-hoc broadening parameters. As can be observed in Figs. 5 and 6, the lines within $\nu_5+\nu_9-\nu_9$ and ν_8 Q branches strongly overlap and the rotational structure vanishes even at low pressures. In this case, the Q branch shape is mainly governed by its equivalent broadening parameter [31] given by

$$\bar{\gamma}^{\mathrm{LM}}_{\mathrm{branch}} = \mathrm{Re}\left\{ \sum_{\ell,k\in\mathrm{branch}} \rho_\ell d_k d_\ell W_{k\ell} \Big/ \sum_{\ell\in\mathrm{branch}} \rho_\ell d_\ell^2 \right\}. \tag{12}$$

Due to the off-diagonal real elements of **W**, this broadening is smaller than that predicted by the isolated lines model. We can thus artificially reproduce line-mixing effects by using Lorentzian line shapes where the line-broadening coefficients are smaller than that of isolated lines. For this purpose, we have multiplied the line-broadening coefficient by a factor smaller than unity, and it is determined by comparisons between observed and calculated spectra. For the ν_8 Q branch line, its value is 0.77. For the $\nu_5+\nu_9-\nu_9$ Q branch lines, it is 0.66, not for all the lines in the branch but only for those belonging to the spectral interval from 885.40 to 885.45 cm^{-1}. In fact, as shown in Fig. 7, unlike the case of the ν_8 Q branch where lines attribution is regular as function of the wavenumber, in the case of the $\nu_5+\nu_9-\nu_9$ Q branch, lines outside this spectral region (885.40–885.45 cm^{-1}) are weak compared with the lines belonging to this interval and they are far enough to consider that they do not contribute appreciably to the line-mixing effect in the band. In order to prove the consistency of this approach, comparisons between measurements and calculations accounting for line-mixing effects using our model (Eqs. (4)–(11)) and using equivalent Lorentzian line shapes are shown at different pressures in Fig. 8 for the $\nu_5+\nu_9-\nu_9$ Q branch. A similar result is obtained for the ν_8 Q branch.

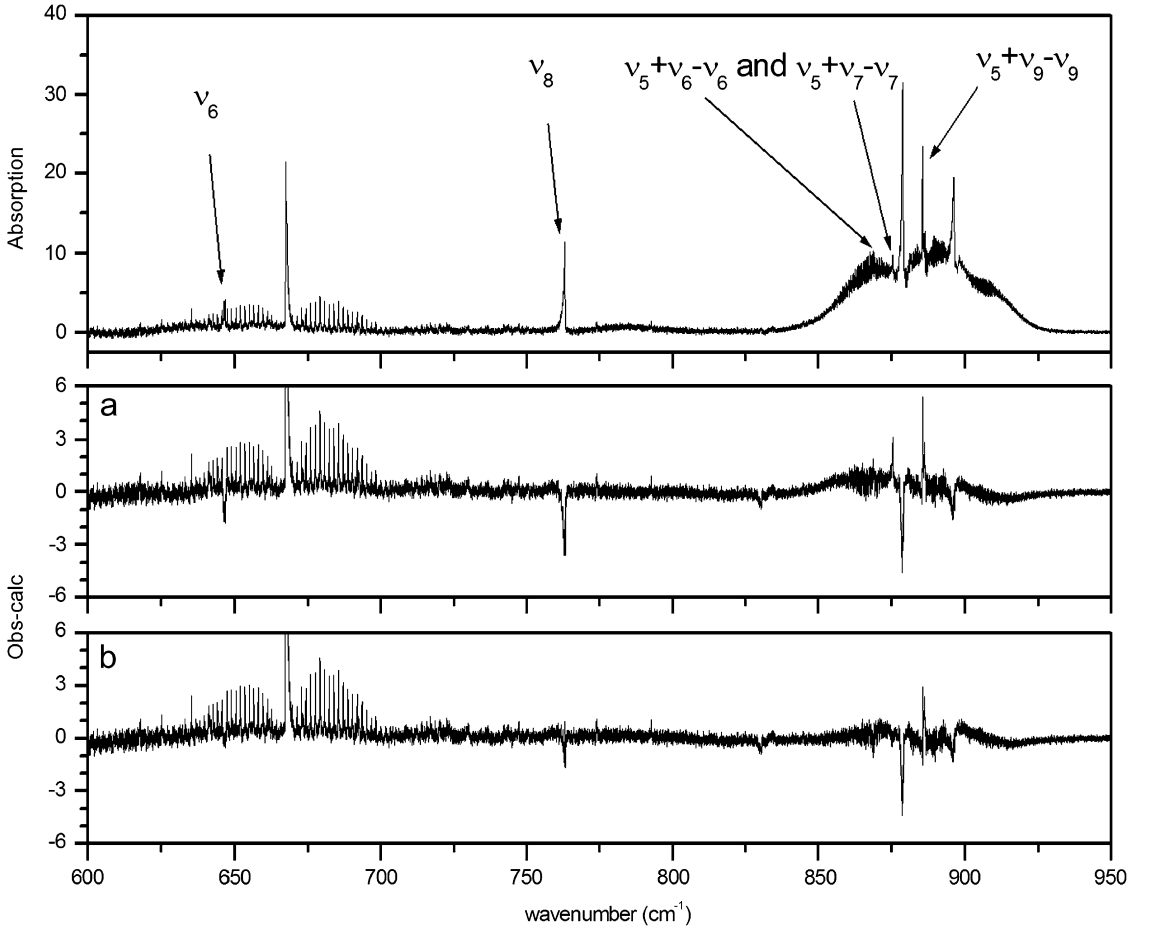

Fig. 9. Absorption of HNO_3 diluted in N_2 measured at 885 hPa and 296 K. Differences between measurement and calculation using (a) the old database and (b) our new database are plotted in lower layers. Regions with improvements thanks to our new database are shown by an arrow.

Please cite this article as: Gomez L, et al. Some improvements of the HNO_3 spectroscopic parameters in the spectral region from 600 to 950 cm^{-1}. JQSRT (2008), doi:10.1016/j.jqsrt.2008.07.004

Finally, in Fig. 9 we show the spectrum measured at 885 hPa in the whole spectral region studied in this work and the differences between measured values and calculations obtained from HITRAN parameters and from our new database.

4. Conclusion

A new and improved HNO_3 database was generated by analyzing spectra of nitric acid broadened by N_2 recorded in the 600–950 cm^{-1} region with a spectral resolution of 0.013 cm^{-1} using the Bruker IFS 125 HR FTIR of the LISA laboratory. During this study, two hot bands $\nu_5+\nu_6-\nu_6$ and $\nu_5+\nu_7-\nu_7$ located at 869.1 and 875.7 cm^{-1} were included in this new database. The intensities were updated for the ν_6 and ν_8 bands at 646.8 and 763.1 cm^{-1}, respectively. The line-broadening parameters were updated using a new calculation. Also it was possible to identify, for the first time, and model correctly line-mixing effects in the Q branch regions of the $\nu_5+\nu_9-\nu_9$ (at 885.425 cm^{-1}) and ν_8 (at 763.154 cm^{-1}) bands. These new parameters will improve the quality of the atmospheric spectra calculations and retrievals in the 10–16 μm region, as will be demonstrated in a forthcoming paper.

Acknowledgments

The authors are indebted to the European Community for financial support within the "QUASAAR" (QUAntitative Spectroscopy for Atmospheric and Astrophysical Research) network project (Contract MRTN-CT-2004- 512202). They also gratefully acknowledge a financial support from the French research program "Les Enveloppes Fluides et l'Environnnement, Chimie Atmosphérique" (LEFE-CHAT) from the "Institut National des Sciences de l'Univers" (INSU). C.E. Fellows was Invited Professor at the Université Paris-Est (Faculty of Sciences and Technology) in 2007.

References

[1] Molina LT, Wang FC-Y. Antarctic stratospheric chemistry of chlorine nitrate, hydrogen chloride, and ice: release of active chlorine. Science 1987;238(4831):1253–1257.
[2] Ridolfi M, Carli B, Carlotti M, von-Clarmann T, Dinelli BM, Dudhia A, et al. Optimized forward model and retrieval scheme for MIPAS near-real-time data processing. Appl Opt 2000;39(8):1323–40.
[3] Russell JM, Farmer CB, Rinsland CP, Zander R, Froidevaux L, Toon GC, et al. Measurements of odd nitrogen compounds in the stratosphere by the ATMOS experiment on Spacelab3. J Geophys Res 1988;D93:1718–36.
[4] Oelhaf H, Von Clarmann T, Fischer H, Friedl-Vallon F, Frizsche Ch, Linden A, et al. Stratospheric $ClONO_2$ and HNO_3 profiles inside the Arctic vortex from MIPAS-B Limb Emission Spectra obtained during EASOE. Geophys Res Lett 1994;21:1263–6.
[5] Camy-Peyret C, Payan S, Jeseck P, Té Y, Acad CR. Mesures spectroscopiques de constituants et de polluants atmosphériques par techniques in situ et à distance, au sol ou embarquées. Sci Paris Ser 2001;IV(2):905–22.
[6] Perrin A, Flaud JM, Camy-Peyret C, Goldman A, Rinsland CP, Gunson MR. Identification of the HNO_3 $3\nu_9-\nu_9$ band Q branch in stratospheric solar occultation spectra. JQSRT 1994;52(3/4):319–22.
[7] Flaud JM, Brizzi G, Carlotti M, Perrin A, Ridolfi M. MIPAS database: validation of HNO_3 line parameters using MIPAS satellite measurements. Atmos Chem Phys 2006;6:1–12.
[8] Rothman LS, Jacquemart D, Barbe A, Chris Benner D, Birk M, Brown LR, et al. The HITRAN 2004 molecular spectroscopic database. JQSRT 2005;96:139–204.
[9] Jacquinet-Husson N, Scott NA, Chédin A, Crépeau L, Armante R, Capelle V, et al. The Geisa Spectroscopic Database: current and future archive for Earth's planetary atmosphere studies. JQSRT 2008;100:1043–59.
[10] Perrin A, Flaud JM, Keller F, Goldman A, Blatherwick RD, Murcray FJ, et al. Analysis of the $\nu_8+\nu_9$ band of HNO_3: line positions and intensities, and resonances involving the $v_6 = v_7 = 1$ dark state. J Mol Spectrosc 1999;194:113–23.
[11] Perrin A, Orphal J, Flaud JM, Klee S, Mellau G, Mäder H, et al. New analysis of the ν_5 and $2\nu_9$ bands of HNO_3 by infrared and millimeter wave techniques: line positions and intensities. J Mol Spectrosc 2004;228:375–91.
[12] Chackerian C, Sharpe SW, Blake TA. Anhydrous nitric acid integrated absorption cross sections: 820–5300 cm^{-1}. JQSRT 2003;82:429–41.
[13] Goyette TM, Ebenstein WL, DeLucia FC. Pressure broadening of the millimeter and submillimeter wave spectra of nitric acid by oxygen and nitrogen. J Mol Spectrosc 1988;128:108–16.
[14] Goyette TM, Guo W, DeLucia FC, Helminger P. Variable temperature pressure broadening of HNO_3 in the millimeter wave spectral region. JQSRT 1991;46(4):293–7.
[15] Goyette TM, Cohen EA, DeLucia FC. Pressure broadening of HNO_3 by N_2 and O_2: An intercomparison of results in the millimeter wave region. JQSRT 1998;60(1):77–84.
[16] Zu L, Hamilton PA, Davies PB. Pressure broadening and frequency measurements of nitric acid lines in the 683 GHz region. JQSRT 2002;73:545–56.
[17] Colmont JM, Bakri B, Rohart F, Wlodarczak G. Experimental determination of pressure-broadening parameters of millimeter-wave transitions of HNO_3 perturbed by N_2 and O_2, and of their temperature dependences. J Mol Spectrosc 2003;220:52–7.
[18] Cazzoli G, Dore L, Puzzarini C, Bakri B, Colmont JM, Rohart F, et al. Experimental determination of air-broadening parameters of pure rotational transitions of HNO_3: intercomparison of measurements by using different techniques. J Mol Spectrosc 2005;229:158–69.
[19] Perrin A, Puzzarini C, Colmont JM, Verdes C, Wlodarczak G, Cazzoli G, et al. Molecular line PARAMETERS for the "MASTER" (Millimeter Wave Acquisitions for Stratosphere/Troposphere Exchange Research) database. J Atmos Chem 2005;51:161–205.
Q1 [20] Laraia A, Gamache RR, Hartmann JM, Perrin A, Gomez L. Calculations of N_2 pressure-broadened half widths for HNO_3. JQSRT, in preparation.
[21] Orphal J, Fellows CE, Flaud JM. The visible absorption spectrum of NO_3 measured by high-resolution Fourier-transform spectroscopy. J Geophys Res 2003;D108(D3):4077.
[22] McGraw GE, Bernitt DL, Hisatsune IC. Vibrational spectra of isotopic nitric acids. J Chem Phys 1965;42(1):237–44.
[23] Perrin A. Recent progress in the analysis of HNO_3 spectra. Spectrochim Acta, part A 1998;54:375–93.
[24] Perrin A, Mbiaké R. The ν_5 and $2\nu_9$ bands of the ^{15}N isotopic species of nitric acid ($H^{15}NO_3$): line positions and intensities. J Mol Spectrosc 2006;237:27–35.
[25] De Bievre P, Holden NE, Barnes IL. Isotopic abundances and atomic weights of the elements. J Phys Chem Ref Data 1984;13:809–91.
[26] Goldman A, Rinsland CP, Perrin A, Flaud JM. HNO_3 line parameters: 1996 HITRAN update and new results. JQSRT 1998;60(5):851–61.

Please cite this article as: Gomez L, et al. Some improvements of the HNO_3 spectroscopic parameters in the spectral region from 600 to 950 cm^{-1}. JQSRT (2008), doi:10.1016/j.jqsrt.2008.07.004

[27] Giver LP, Valero FPJ, Goorvitch D, Bonomo FS. Nitric-acid band intensities and band-model parameters from 610 to 1760 cm^{-1}. J Opt Soc Am B Opt Phys 1984;1(5):715–22.
[28] Wang WF, Looi EC, Tan TL, Ong PP. Line intensities in the ν_8 band of HNO_3. J Mol Spectrosc 1996;178(1):22–30.
[29] Tan TL, Wang WF, Looi EC, Ong PP. High resolution FTIR spectrum of the ν_6 band of HNO_3. Spectrochim Acta, PartA, Mol Biomol Spectrosc 1996;52A(10):1315–7.
[30] Looi EC, Lan TL, Wang WF, Ong PP. Improved spectroscopic constants for the ν_7 and ν_8 bands of HNO_3. J Mol Spectrosc 1996;176(1):222–5.
[31] Hartmann JM, Boulet C, Robert D. Collisional effects on molecular spectra: laboratory experiments and models, consequences for applications. Amsterdam: Elsevier; 2008.
[32] Tran H, Jacquemart D, Mandin JY, Lacome N. Line mixing in the ν_6 Q branches of self- and nitrogen-broadened methyl bromide. JQSRT 2008;109:119–31.
[33] Rodrigues R, De Natale P, Di Lonardo G, Hartmann JM. Line-mixing effects in the rotational ^rQ-branches of $^{16}O_3$ perturbed by N_2 and O_2. J Mol Spectrosc 1996;175:429–40.
[34] Flaud JM, Perrin A, Orphal J, Kou Q, Flaud PM, Dutkiewicz Z, et al. New analysis of the $\nu_5+\nu_9-\nu_9$ hot band of HNO_3. JQSRT 2003;77:355–64;

Please cite this article as: Gomez L, et al. Some improvements of the HNO_3 spectroscopic parameters in the spectral region from 600 to 950 cm^{-1}. JQSRT (2008), doi:10.1016/j.jqsrt.2008.07.004